3.8 Beam Delivery

A schematic of the beam delivery and removal systems is shown in Fig. 3.3. These systems begin at the end of the linac and terminate at a post-IP beam dump. The total linac-to-IP length is 5.2 km. They include a post-linac collimation system, an IP switch and big bend, a pre-final-focus diagnostic and skew-correction section, a final-focus system, and a post-IP beam line. The design of all of these systems has been strongly influenced by experience with similar systems at the SLC.

Figure 3.23 shows the lattice β functions from the linac to the IP for the 1-TeV cms beam line. The first 100 meters contain a post linac diagnostic chicane, which is then followed by a 2.5-km collimation system. The maximum β-function points in the collimation region correspond, for the most part, to the location of horizontal collimators and chromatic correction sextupoles. The horizontal β-function peak at 2.6 km marks the location of the IP switch. After that, up to the 3.0-km marker, is a small β-function region that contains the big (10 mrad) bend, and following this, up to the 3.4-km marker, is a small β-function region containing a pre-final-focus diagnostic and skew-correction region. In this region beam sizes in all phases and planes can be measured and the presence of coupling detected and corrected. The region from 3.4 km to 3.8 km contains the β match into the final focus. Following the β match, the first two peaks are the positions of the horizontal chromaticity compensation sextupoles. The last peak, in each plane, at the end of the beam line, is located at the position of the final-doublet elements.

We have studied beam delivery systems for center-of-mass energies from 350 GeV to 1.5 TeV, for a broad range of assumptions on beam and IP parameters, and have shown that it is possible to meet system specifications over this entire range. Within this energy span, the final-focus system design we have chosen requires two minor upgrades consisting of a transverse displacement of magnets by 20 cm or less and a change of the final doublet. The tunnel length allotted to collimation is adequate to collimate energy and the horizontal and vertical planes at both phases only one time at 1.5 TeV cms energy. Since the centroid orbit of the collimation system differs only slightly from a straight line, it would be possible to allocate length at the end of the linac tunnel for a second IP phase collimation at this energy. It is sufficient to collimate the final doublet (FD) phase only one time.

3.8.1 Collimation System

The design of the post-linac collimation is strongly influenced by assumptions on incoming beam conditions. The number of particles needing to be collimated is difficult to predict precisely, because it depends on how well upstream systems have been tuned; we have relied on SLC experience for this estimate. Downstream, the number of particles that can be collimated in the final-focus system can be determined by edge-scattering and muon transport studies. The rough guideline that evolves from these considerations is that for each bunch train there may well be a few times 10^{10} particles per bunch train in the tails at the end of

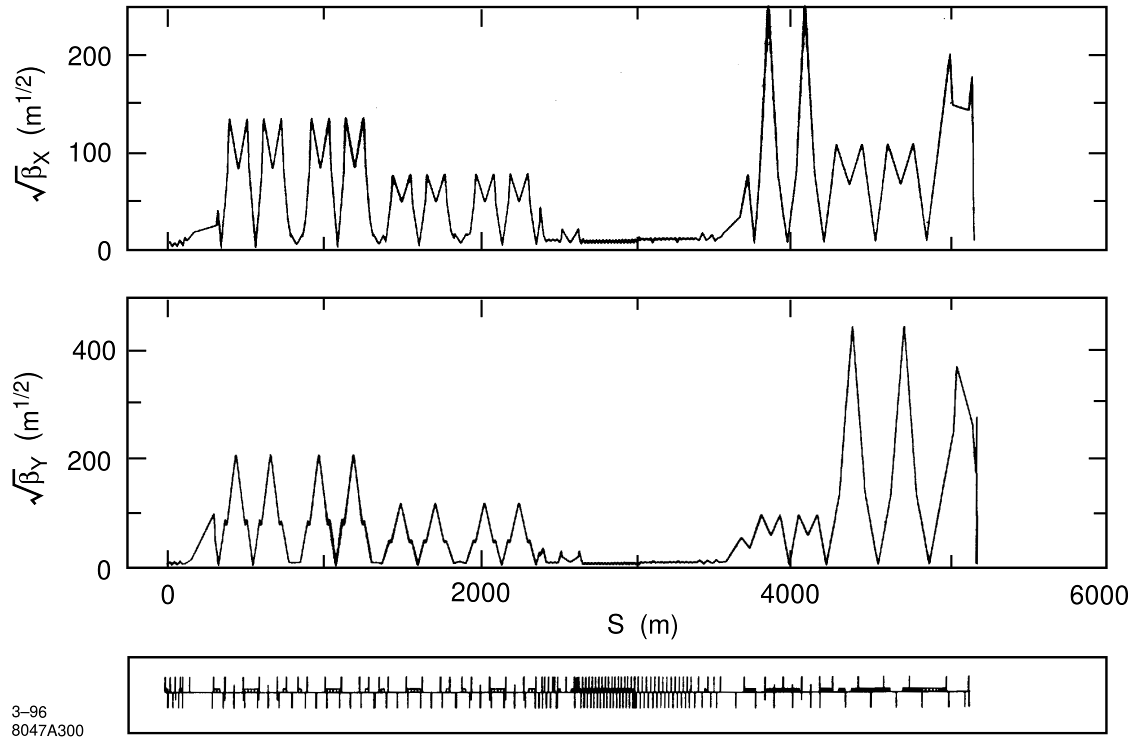

Figure 3.23: The β functions from the linac to the IP for the 1-TeV cms beam line.

the linac. This number needs to be reduced to a few times 10^6 upon entry into the final-focus system.

Two types of collimation systems have been proposed: linear and nonlinear. In the former, beam enlargement at the collimators is achieved by traditional linear optics methods; in the latter strong sextupoles are used to blow up the beam. Since the sextupoles are exceedingly strong and system lengths are not reduced in the specific system proposals we have studied, we have opted to look in depth at a linear collimation scheme. It is not precluded that a nonlinear (or combination linear and nonlinear) system could be found that would be operationally superior and have a lower total cost. Our primary objective in the ZDR was to show that at least one collimation system exists that fulfills all functional requirements.

Since a small perturbation in upstream conditions could cause a complete bunch train of 10^{12} particles to be incident on the collimators of the collimation system, it is necessary in both the linear and nonlinear systems to rely on a primary collimator that is a spoiler, followed by a secondary collimator which is the absorber. The function of the spoilers is to increase the angular divergence of the beam, so that when the beam arrives at the absorber it has a much larger size (2.2 mm radius). The spoilers must be thermally rugged and very thin (1/4 radiation length). The best material we have found is a titanium alloy plated with titanium nitride for better electrical conductivity. The absorber, on the other hand,

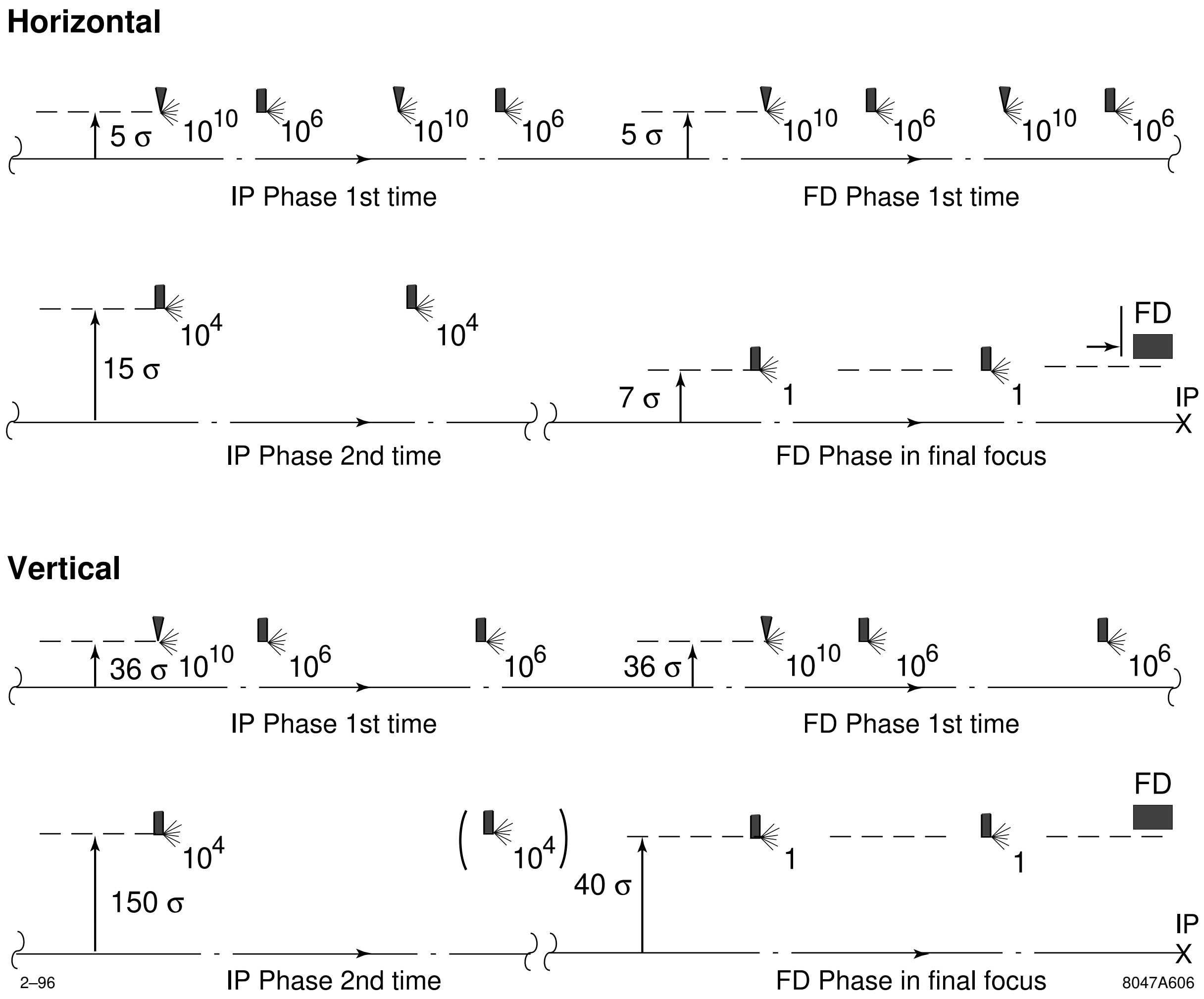

Figure 3.24: A schematic of the collimation system spoilers and absorbers. The apertures are shown as well as the estimated number of tail particles rescattered into the beam.

must be able to routinely absorb and remove the full energy in the beam tail. For the 1 TeV cms parameters, 1% of the time-averaged beam power is 84 kW. The preferred material for absorbers is copper. Figure 3.24 is a schematic of all spoilers and collimators in the beam delivery system. This figure shows the apertures and estimates for the number of tail particles rescattered into the beam.

The wake fields of the collimators can have a very deleterious effect on the beam core. To minimize the wakes, the beam pipe must be tapered before and after the collimator. A parallel-plane collimator will have a quadrupole wake even for an on-axis beam core, which can cause focusing of the core and alter the trajectory of particles in the tails. And beams that have been mis-steered close to the wall can experience very large wake-induced kicks. Because of the latter effect, the aperture of the second stage of IP-phase collimation must be quite large. This in turn places a requirement on the transmission quality of the beamline from the collimation system to the final-focus system, and on the dynamic aperture of the final-focus system. These have been verified with tracking studies.

Because of the large β-functions and strong focusing that arise when the beam is blown up with linear optics, there are important chromatic effects to compensate with sextupole pairs. And because it is necessary to collimate each transverse phase at least one time, there are very large R_{12} and R_{34} functions within the system. Large R_{12} and R_{34} functions lead to tight tolerances. Stability tolerances, that must be held between tunings of the waist knobs in the final-focus system, are looser than stability tolerances within the final-focus system. Though the particle backgrounds in the collimation system preclude the beam-based stabilization methods contemplated for the final-focus system, beam changes can be monitored non-invasively in the skew correction system and aberrations arising from changes in the collimation system can be continuously compensated there.

Ground motion studies show that seismic ground motion in the beam delivery system has a negligible impact on beam collision offsets at the IP. As a result, vibration tolerances become tolerances between beam-line elements and the ground beneath them (FFTB quadrupoles mounted on movers have been shown to follow the ground $\pm$ 1 nm), or tolerances on ground motion coming from cultural sources.

In the ZDR we have described the system specifications, discussed the relevant properties of materials, presented spoiler and edge-scattering distributions, clarified the relevant wake-field of tapered collimators and defined the optimum choice of collimator shape, quantified the impact of near-wall wakes for on-axis and mis-steered beam, designed lattices that implement the required functionality, calculated the position and strength tolerances of the magnetic elements, clarified the impact of ground motion, tracked the lattices to confirm their functionality, tracked spoiler distributions in the collimation system to determine power deposition, tracked edge-scattered distributions in the final-focus system to determine the probability of particle impacts on the final doublet, determined the extent of tail repopulation due to gas scattering, discussed potential operational problems, and addressed machine protection issues. To our knowledge all issues have been addressed with the satisfactory conclusion that it is possible to build and operate a collimation system for the proposed beam parameters from beam energies of 175 GeV to 750 GeV, that will collimate the beam at the apertures required by the final-focus system. We believe that we have demonstrated an existence proof.

3.8.2 IP Switch and Big Bend

Following the collimation system are the IP switch, the big bend, and the skew correction and diagnostic section, as illustrated in Fig. 3.3. An NLC design with two IPs will require two IP switches and four big bends.

The IP switch follows the main linac and collimation section and allows slow switching between multiple IPs. It bends the beam a total of 1.5 mrad. Figure 3.25 shows the IP switch optics. The QS quadrupole is horizontally movable in order to switch between IPs. It is displaced by ± 3.25 cm (± 2.6 cm) for the 500-GeV per beam (750-GeV per beam) configuration.

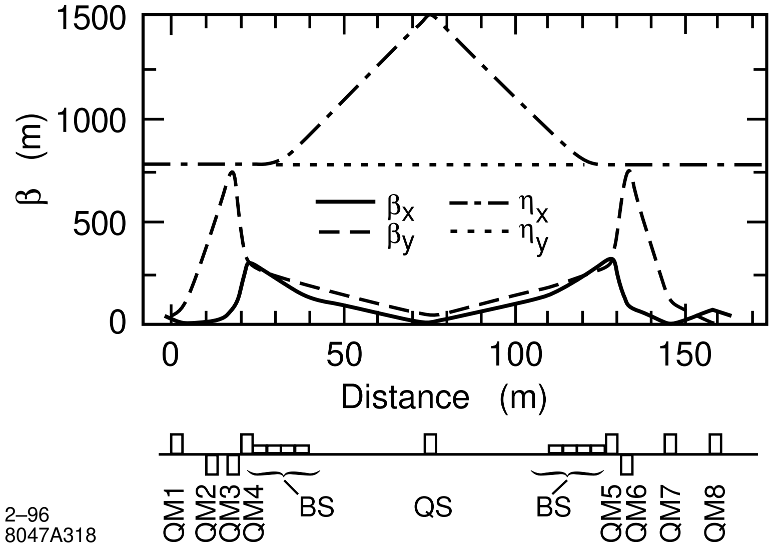

Figure 3.25: IP Switch Optics (500 GeV per beam).

The big bend is a low-angle arc after the main linac which provides detector muon protection, IP separation, and an IP crossing angle to facilitate extraction of the spent beams. The total bend angle (including 1.5-mrad IP switch angle) is 10 mrad (20-mrad IP crossing angle) which provides approximately 40-m spatial separation between the two IPs (approximately 700-m transport to an approximately 1600-m-long final focus). At 500–750 GeV per beam, the horizontal emittance growth due to SR sets lower limits on the system design length. The optical design of the big bend section was optimized for 500 GeV per beam and 750-GeV per beam electrons (or positrons). The total emittance growth (in both IP switch and big bend) for the optimized design, due to chromatic filamentation and due to synchrotron radiation, is less than 2% vertically and 3% horizontally, for a beam energy of

500 GeV. The big bend rotates the spin orientation by about 550° at 500 GeV. The relative depolarization is small: 0.06% for a 0.3% energy spread.

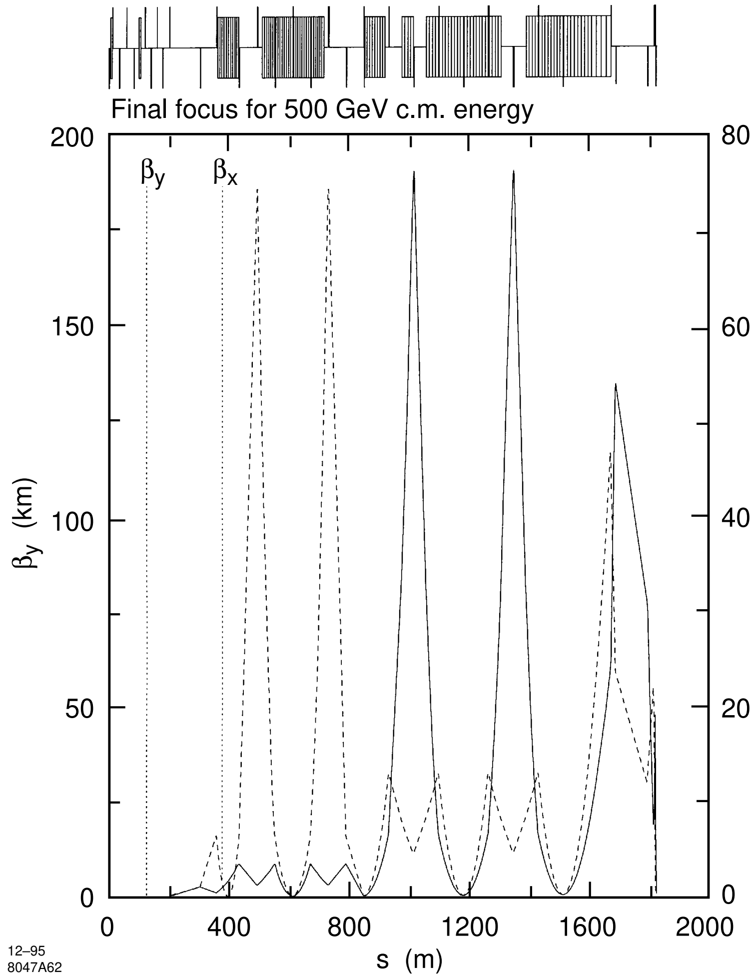

Figure 3.26: Horizontal and vertical beta functions for the 500-GeV final focus.

3.8.3 Final Focus

The main purpose of the NLC final-focus system is to transport electron and positron beams of energy 180 GeV to 750 GeV from the end of the big bend to the IP, where the demagnified beams are collided with a typical spot size of 4–8 nm vertically and 200–300 nm horizontally. One must also remove the beam remnants cleanly in order to facilitate crucial post-IP diagnostics.

The basic layout of the final focus is very similar to that of the Final-Focus Test Beam (FFTB). The final focus is constructed from six functional modules. These are, in the order of their location: geometry-adjustment section (GAS), beta- and phase-matching section (BMS), horizontal chromatic correction section (CCX), beta-exchanger (BX), vertical chromatic correction section (CCY), and final transformer (FT). The total distance from the entrance of the GAS to the IP is about 1820 m. A schematic of the magnet configuration is depicted in the top part of Figure 3.26. The figure also shows the beta functions corresponding to the largest IP beam divergences of the NLC parameter plane, for which the system was designed. This represents a worst case, since the effect of nonlinear aberrations, the aperture requirements, and the Oide effect (synchrotron radiation in the last quadrupoles) all become more severe for larger divergence. Located at the end of the final transformer is the final doublet, which focuses the beam to the design spot size at the IP. In the NLC, the final doublet is actually a quartet comprising four different quadrupoles: 2 conventional magnets, 1 superconducting and 1 permanent.

The chromaticity (energy-dependent focusing) of the final doublet is similar to that at the FFTB, and about 5 times larger than in the SLC. If the chromaticity were not corrected, the vertical IP spot size would increase by about a factor of 100 from the design value. The chromatic correction is accomplished in two separate beam-line sections, CCX and CCY, each of which accommodates a pair of sextupoles separated by an optical transform ($-I$) that cancels geometric aberrations and second order dispersion. The momentum bandwidth of the final focus was optimized with three additional sextupoles and exceeds ± 0.6 %.

The NLC design calls for a 20-mrad crossing angle of the two beams at the IP, which requires two separate beam lines. Magnet apertures and focusing strengths in the two beam lines can be chosen independently, and are in fact quite different. The crossing angle, furthermore, requires rotation each beam prior to collision by 10 mrad in the horizontal/longitudinal plane, by means of a 5-cm-long X-band crab cavity.

Placed about 150 m in front of the final doublet is a 70-m long soft bending section with a 12-G field, which serves to deflect the beam orbit at the final-doublet entrance by about 8 mm with respect to the hard photons radiated upstream, and, thereby, reduces the detector background substantially. A similar soft bend has proved invaluable at the SLC.

The final focus can operate in the entire cms energy range between 350 GeV and 1.5 TeV. This flexibility is achieved with three slightly different geometries, illustrated in Fig. 3.27. A dedicated geometry-adjustment section (GAS) at the entrance to the final focus is used to adjust the incoming beam-orbit angle for the different geometries, such as to keep the IP position constant and the transverse magnet displacements small. Energy adjustability of the final doublet is provided by the superconducting quadrupole, whose field changes sign when the beam energy is raised from 250 GeV to 500 GeV. Finally, the apertures of all magnets are consistent with a minimum vertical beam stay-clear of $55\sigma_y$ at 500-GeV cms energy.

Higher-order optical aberrations, synchrotron radiation, residual uncorrected low-order aberrations, timing offsets and crab crossing errors all reduce the luminosity. A total luminosity loss of about 30% is included in the NLC design parameters. The low-order aberrations, such as dispersion, waist shift, skew coupling, *etc.*, which are responsible for almost half of

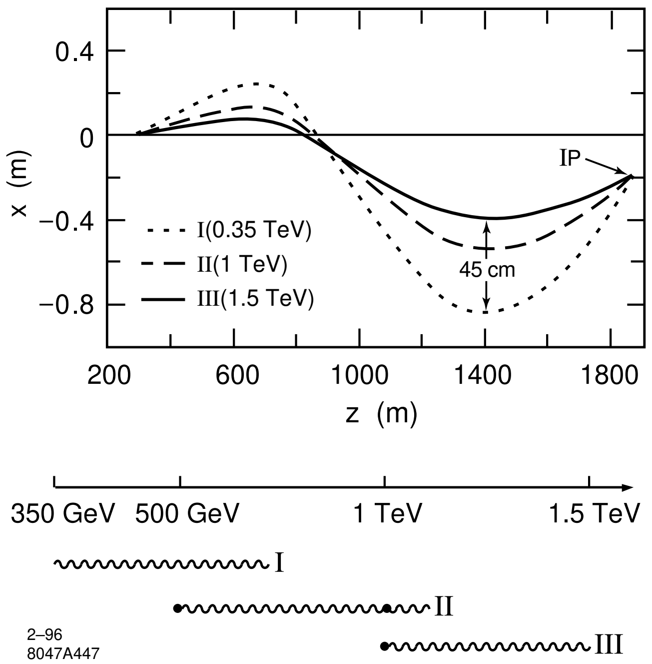

Figure 3.27: Top view of the final focus, and energy range of the three different geometries. Magnet displacements by at most 45 cm are necessary during an upgrade from 500 (350) GeV to 1.5 TeV, while the IP-orbit angle changes by about 1.5 mrad.

the total loss, need to be tuned and corrected at regular intervals, *e.g.*, every few hours. An average luminosity loss of 1–2% was assumed for each low-order aberration. Actual tuning accuracy in the SLC is about 0.5%.

The design luminosity is achieved, if, first, the aberrations stay small between tunings, and, second, the beams collide head-on at the IP (rms offset smaller than a quarter of half the beam size). The first condition translates into tolerances on magnet-position drifts over a 1-s time scale and on BPM stability over a few hours. The FFTB magnets and BPMs fulfill all the NLC tolerances. The second condition is met, when a) the effect of ground motion is not important and b) the magnet vibrations with respect to ground are reasonably small.

The ground motion measured above 0.01 Hz can be explained by isotropic plane ground waves, for which each frequency is associated with a certain wavelength; longer wavelengths correspond to lower frequencies. Figure 3.28 shows the response of the NLC final focus to a harmonic vertical displacement of quadrupoles as a function of wavelength. Plotted is the average squared ratio of the IP beam-beam offset and the ground-motion amplitude. The figure illustrates that the effect of ground motion is heavily suppressed at long wavelengths, *i.e.* below about 2 Hz ($k \leq 0.01$ m^{-1}). To calculate the expected beam-beam offset at the IP, one has to convert the curve of Fig. 3.28 into frequency domain, and, after multiplication with the ground-motion frequency spectrum and a typical SLC feedback response curve (see Fig. 3.29), to integrate over frequency. The total luminosity loss due to ground motion is then

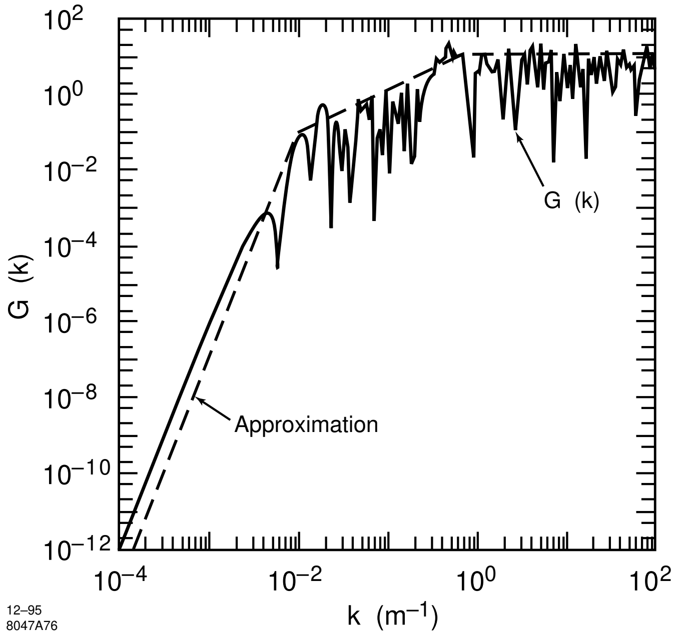

Figure 3.28: Lattice response function for the NLC final focus system.

predicted to be 0.8% on the SLAC site, and 0.02% at a quiet site (*e.g.* LEP tunnel). An upper bound on the luminosity loss due to any additional uncorrelated ground motion is 0.04%. The conclusion is that one can use the ground (bedrock) as a reference for stabilization.

Thus magnet supports need to be designed which neither amplify nor damp the ground motion, but couple the magnet firmly to the ground. At DESY (SBLC-TF), the rms relative quadrupole-to-ground vibrations above 1 Hz were measured to be smaller than 1 nm, which would meet all the NLC tolerances. Quadrupoles at the FFTB were found to vibrate by about 4 nm with respect to the ground, excited mainly by bad cooling pumps. These vibration amplitudes would still satisfy the tolerance criteria for all NLC magnets other than the final doublet. For the latter a special stabilization system based on an optical anchor and piezo-electric movers has been devised, which is discussed in the following chapter.

The beam extraction line behind the IP guides the disrupted beam onto a water-based beam dump, which must dispose of all the beam power (about 10 MW). Numerous diagnostics in the extraction line allow to control and stabilize beam orbit and energy, and also to monitor luminosity and polarization. A schematic is depicted in Fig. 3.30.

In conclusion, the NLC beam delivery system will not only produce small spot sizes at the IP, but it also promises redundant tunability, adjustability over a wide energy range, and a tolerable detector background. Most tolerances on magnet strength or position stability are not particularly tight, and have, in fact, already been achieved at the FFTB or at other places. Also natural ground motion is not thought to be a problem. However care is needed in the mechanical design of components and supports.

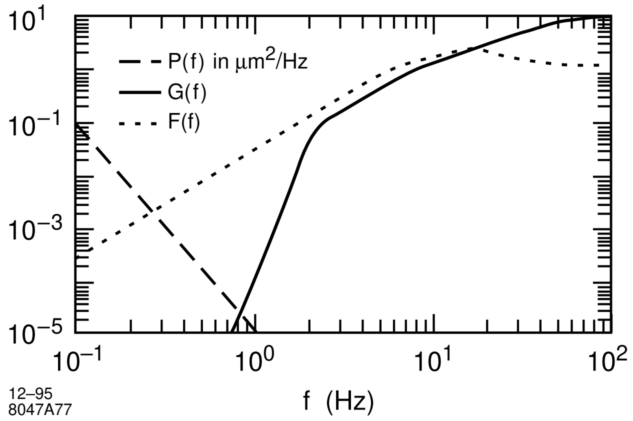

Figure 3.29: Three functions which determine the rms beam-beam separation due to plane-wave ground motion: $F(f)$—the feedback response; $P(f)$—the local power density; $G(f)$—the lattice response function converted into frequency domain. The integral over the product of these functions gives the square of the rms beam-beam separation.

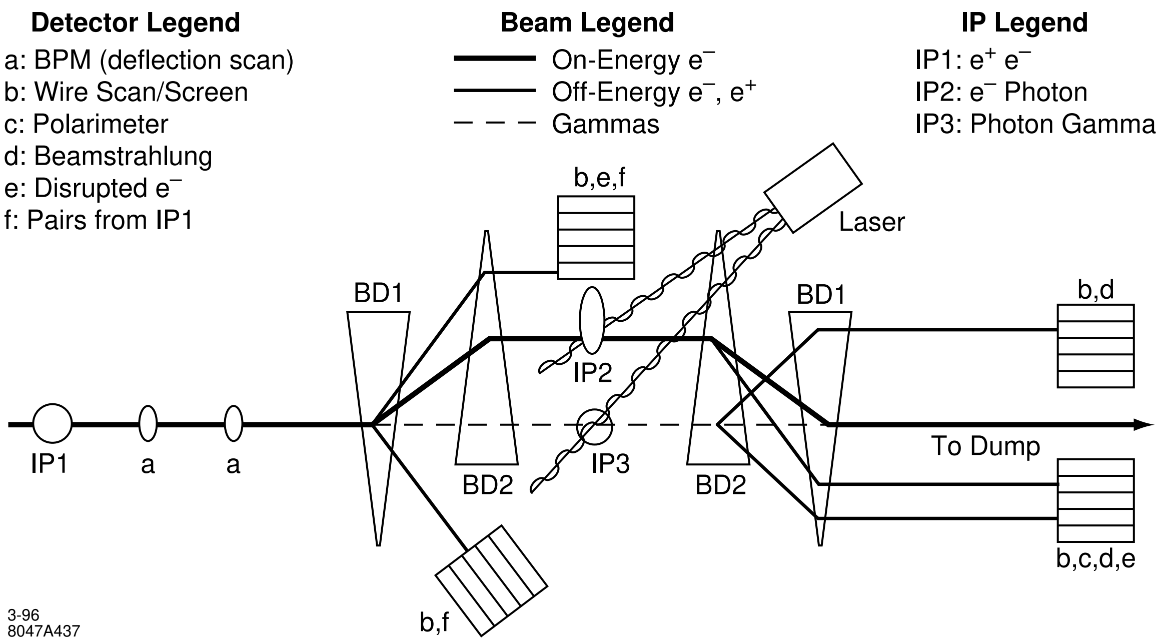

Figure 3.30: NLC Extraction Line and Diagnostic Layout.